

Proceedings of the ASME-JSME-KSME 2019 8th Joint Fluids Engineering Conference AJKFluids2019 July 28-August 1, 2019, San Francisco, CA, USA

AJKFluids2019-5499

CHARACTERIZATION OF AGGREGATE DISRUPTION USING ORGANIC MARINE PARTICLES AND PARTICLE TRACKING MEASUREMENTS IN ROTATING/OSCILLATING AGGREGATION TANKS

Yixuan Song, Matthew J. Rau¹
Mechanical Engineering
The Pennsylvania State University
University Park, PA 16802, USA

ABSTRACT

The fate of particulate matter in the ocean is determined in large part by its size and settling rate. Disaggregation, caused by turbulence-induced shear, acts to fracture or erode large particles into slower-settling sub-aggregates and primary particles. The strength and breakup response of organic marine aggregates (i.e. marine snow particles consisting of phytoplankton) is poorly understood, limiting our ability to accurately predict marine particle transport effects on the global carbon cycle. A study was conducted to enable the investigation of disaggregation effects on these organic marine particle aggregates. Due to the fragile nature of the Phytoplankton cells and their resulting aggregates, test facilities that do not rely on external sampling or pumps are required. A novel rolling aggregation tank was developed that can both aggregate phytoplankton cells under varying hydrodynamic conditions and then expose them to calibrated shear forces using laminar oscillating flow. The theory behind the operation of this tank is presented along with the necessary operating conditions to create stable regions within the tank where particle settling effects are minimal but shear is still representative of values expected in the open ocean. Phytoplankton was cultured in the laboratory to create simulated marine snow particles in the open ocean for disaggregation experiments. The procedure to calculate and track the shear-history of each aggregate is described and how the data generated from this facility will be used to quantify disaggregation parameters relevant for population balance modeling is discussed.

Keywords: Particle aggregation, disaggregation, roller tanks, population balance.

NOMENCLATURE

a	rotation component of wall velocities
b	amplitude of oscillation
C_S	empirically-derived strength parameter
d	relevant aggregate lengthscale
m	mass
r_0	balance length of standard roller tank
r_s	radius of stable region
A	aggregation process
A_i	rate at which smaller particles aggregate into
	larger clusters of mass m
A_o	rate at which aggregates of mass m disrupt into
	smaller particles
B	breakup process
B_i	rate at which larger aggregates break into
	smaller sub-aggregates or particles of mass m
B_o	rate at which aggregates of mass m disrupt into
	even smaller particles
K	breakup frequency
R	radius of roller tank
S_{io}	sources or sinks of particulate mass
W	gravitational settling
u_s	particle sinking velocity
α	particle stickiness parameter
β	aggregation kernel
γ	shear rate
ε	energy dissipation rate
$\mathcal{E}b$	dissipation rate that causes disruption of an

aggregate of mass m

¹ Contact author: matthew.rau@psu.edu

θ phase angle λ average eddy frequency ν kinematic viscosity ω frequency of oscillation Γ breakup mass size distribution Ω angular rotation speed of roller tank

INTRODUCTION

Aggregation is the process by which colloidal particles stick together to form larger particle clusters, typically called aggregates or flocs. Disaggregation is the reverse process, where an already-formed aggregate disrupts into sub-aggregates or primary particles. Together, aggregation and disaggregation act to govern particle size and transport properties in diverse applications, including waste-water treatment systems [1], dredging processes [2], fouling in heat exchangers and airhandling equipment [3], drug manufacturing and delivery systems [4], and many others. In the environment, aggregation and disruption are critically important to understanding sediment transport and for predicting particulate carbon transport in the ocean [5]. While aggregation theory has been well-developed, no robust disruption model yet exists that can adequately predict aggregate breakup due to turbulence and its effect on the size, shape, and settling rate of naturally-occurring particle aggregates. This is currently limiting our ability to quantify and predict carbon sequestration rates in the ocean as part of the global ocean carbon pump.

Motivated by the broader goal of developing aggregate disruption models for ocean biogeochemical transport predictions, this work presents the development and implementation of a novel aggregation/disaggregation tank. The tank is specifically designed to cause both aggregation and disaggregation conditions of relevance for organic marine particles without any needed external particle sampling, pumps, or other manipulation that could damage the organic material. The tank, and how it was developed in reference to needed hydrodynamic and disruption parameters, are described in detail below.

1.1 Building a disaggregation model

Aggregation and disruption can be modeled through the one-dimensional population balance equation (PBE) following [6]. The advantage of the PBE over more complex particleresolved models is that it can be easily coupled to larger ocean or computational fluid dynamics simulations for particle transport calculations. The PBE is given by

$$\frac{dN(m,t)}{dt} = A_i - A_o + B_i - B_o + W + S_{io},$$
 (1)

where N is the time-varying number distribution of particles of mass m. The number of particles in a population is governed by aggregation processes (denoted by the A terms), breakup processes (B terms), loss due to gravitational settling (W), and sources or sinks of particulate mass (S_{io}). Particle loss due to gravitation settling is typically defined through terminal velocity

estimates. Source and sink terms can come from a variety of sources but are typically caused by growth and feeding of organisms for organic marine particles.

Aggregation rates depend heavily on particle type and the flow field and are typically modeled as

$$A_{i} = \frac{\alpha}{2} \int_{0}^{m} \beta(m_{j}, m - m_{j}) N(m - m_{j}, t) N(m_{j}, t) dm_{j},$$

$$A_{o} = \alpha N(m, t) \int_{0}^{\infty} \beta(m, m_{j}) N(m_{j}, t) dm_{j},$$
(2)

where A_i denotes the rate at which smaller particles aggregate into larger clusters of mass m while A_o describes the rate at which aggregates of mass m disrupt into smaller particles. Both aggregation rate equations are a function of a particle stickiness parameter (α) and the aggregation kernel (β). The aggregation kernel describes the frequency with which particles come into contact given their relative sizes and the surrounding hydrodynamics. Aggregation kernels are well established for both laminar and turbulent flow in the literature [6].

Disaggregation has seen less agreement in the literature, especially for aggregates consisting primarily of organic material relevant to the open ocean (*i.e.* phytoplankton and other organic microorganisms). The breakup terms of the PBE can be expressed as functions of the particle number distribution as

$$B_{i} = \int_{m}^{\infty} K(m_{j}) \Gamma(m, m_{j}) N(m_{j}, t) dm_{j}$$

$$B_{o} = K(m) N(m, t), \qquad (3)$$

$$where: \int_{0}^{m} m_{j} \Gamma(m, m_{j}) dm_{j} = m$$

In the above equation, B_i is the rate at which larger aggregates break into smaller sub-aggregates of mass m and B_o is the rate at which aggregates of mass m disrupt into even smaller particles. In order to develop disaggregation relationships for use in the PBE, both the breakup frequency of aggregates as a function of their mass (K) and the function describing the size distribution of the breakup mass (Γ) need to be defined for a wide range of hydrodynamic and particle conditions.

1.2 Background and prior efforts

In a turbulent fluid, disaggregation is typically caused by hydrodynamic shear from the surrounding turbulence. Parker *et al.* [7] conducted an early attempt to theoretically define the breakup frequency (K) of aggregates in waste treatment processes. Their model agreed well with experimental data for inorganic aggregates but failed to agree with the measured disruption response of organic aggregates. A key limitation in this study was the assumption that sub-aggregates were not formed during disruption. Instead, only the shearing of primary particles from the aggregate surface was considered. Subsequent studies have often taken an empirical approach to developing aggregate disruption models, with breakup frequency equations being assumed to follow a power-law of the form $K \propto d^b$, where d is a relevant aggregate lengthscale [8,9,10].

A few attempts have been made to theoretically define *K* in equation (3); however, these relationships still typically rely on some *a-priori* knowledge of the aggregate strength. In their study

of clay aggregates, Hsu and Glasgow [1] assumed that the distribution of turbulent eddies in a baffled mixing tank followed a Poisson distribution to derive a breakup frequency of

$$K(m) = \lambda \operatorname{erfc} \left[c_s / (\varepsilon m)^{1/3} \right], \tag{4}$$

where ε is the dissipation rate of turbulence kinetic energy, λ is the average eddy frequency and c_s is an empirically-derived strength parameter. Similarly, Kusters [11] developed a breakup frequency equation of

$$K(m) = \left(\frac{4}{15\pi}\right)^{1/2} \left(\frac{\varepsilon}{v}\right)^{1/2} \exp\left(\frac{-\varepsilon_b(m)}{\varepsilon}\right),\tag{5}$$

where ε_b is the empirically-derived value for the dissipation rate that causes disruption of an aggregate of mass m.

Definition of the size distribution of the breakup mass, Γ , has seen less development in the literature, with various functions having been assumed for implementation into the PBE. These have included the formation of only primary-particles [7], binary aggregate breakage [7,12,13], tertiary breakage [14], and even uniform mass re-distribution [8]. Only recently has high-speed visualization been applied to actively track aggregates and their breakup mass during disruption to statistically quantify the resulting size distribution of their breakup mass [10].

1.3 Goals of this study

The breakup response of organic marine aggregates of relevance to biogeochemical transport predictions in the ocean are under-investigated in the literature. Due to their variability in size, shape, structure, and particle content, models to predict the disruption behavior of these naturally-occurring aggregates will likely remain semi-empirical, requiring some empirical study of the disaggregation behavior of these aggregates. This study presents the design and implementation of a novel aggregation tank for the express study of organic marine particle aggregation and disaggregation. The tank can provide both gentle rolling to simulate aggregation due to differential sedimentation and also expose aggregates to precise amounts of hydrodynamic shear of ranges relevant to the oceanic environment. Design calculations are presented in detail along with a description of the experimental implementation.

METHODS

2.1 Design of an oscillating/rotating tank for the study of disaggregation

Brownian motion, shear forces from laminar or turbulent flow, and differential sedimentation are mechanisms by which particles come into contact and aggregate [15]. Fluid shear and differential sedimentation are most relevant in the marine environment. Shanks and Edmondson [16] introduced the concept of the roller tank to form laboratory-made marine aggregates. Aggregates were formed by flocculation of particles inside a cylinder filled with sea water and rotating with a constant angular speed. After an initial start-up period, shear within the fluid in the tanks dissipates and solid-body rotation of the fluid and particles persists. Any solid particles suspended in

the flow continually settle and aggregate through differential sedimentation. Their design quickly became the standard method to form marine aggregates [17]. The hydrodynamic response of these tanks with time, and their influence on particle aggregate formation, have been described in detail by Jackson [17,18].

When designing a particle aggregation system, it is important that effects of walls, pumps, impellers, etc. are minimized as they may influence the shape, structure, and strength of aggregated particles. Based on analysis of the fluid motion, the trajectory of a falling particle in a roller tank can be traced over time. The velocity of a falling particle is determined by the sum of the particle's sinking velocity and the water velocity at the particle position. For given tank dimensions, rotation rates, and particle settling velocities, it is possible to divide the tank cross-sectional area into stable and un-stable regions. Stable regions are defined as all of the initial particle positions where particles will never come into contact with the wall of the tank. Unstable regions are defined as the initial positions where the particles will eventually hit the tank wall, potentially altering their aggregation state. For tanks with a constant rotation rate, stable regions can be calculated as shown in Figure 1, where Ω is the angular rotation speed of the roller tank, R is the radius of the roller tank and r_s is the radius of our stable region. The balance length, r_0 is obtained from the quotient of the falling velocity and the angular rotation speed ($r_0 = u_s/\Omega$). The equation $r_s = R - r_0$ then indicates the regions of the tank that are stable. The particles that begin in this region will not touch the wall of the roller tank. The area of the stable region compared to the total tank cross-sectional area is then given by $(r_s/R)^2$.

While the standard roller tank design provides a convenient way to aggregate particles through differential sedimentation, no shear forces are present in the fluid once steady solid-body rotation is achieved. We are proposing a modification to the standard design that will allow aggregates to be subjected to fluid shear. In addition to a constant rotation rate, a periodic oscillation is superimposed on the tank motion. This modification not only allows us to form aggregates under a variety of shearing

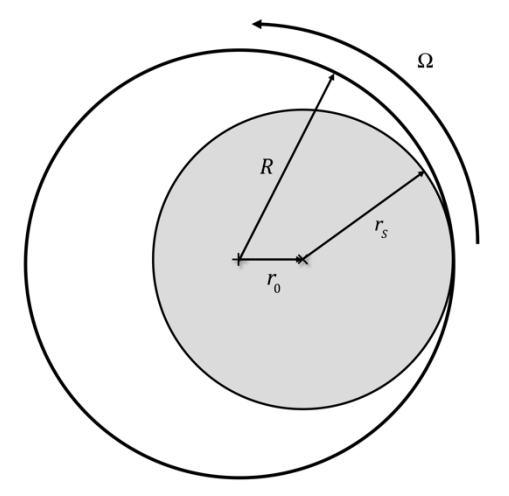


Figure 1. The stable region (shaded) in traditional rotating tanks

conditions in addition to differential sedimentation, but also allows us to expose already-formed aggregates to hydrodynamic shear for disaggregation studies.

2.2 Design procedure

Consider a two-dimensional rotating cylinder filled with water. Using cylindrical coordinates, we can define the velocity vector for a parcel of fluid as (u_r, u_θ, u_z) , where only the angular component of velocity will vary with radial position within the cylinder. The Navier Stokes equation can be reduced to

$$\frac{\partial u_{\theta}}{\partial t} = v \left(\frac{\partial^2 u_{\theta}}{\partial r^2} + \frac{1}{r} \frac{\partial u_{\theta}}{\partial r} - \frac{u_{\theta}}{r^2} \right), \tag{6}$$

where v is the kinematic viscosity of water. If the water in the cylinder begins at rest. The initial and boundary conditions are,

$$u_{\theta}(r,0) = 0$$

$$u_{\theta}(0,t) = 0$$

$$u_{\theta}(R,t) = a + b \cdot \sin(\omega \cdot t)$$
(7)

To create the oscillation condition, we allow the third boundary condition, the no-slip boundary condition on the outer tank wall, to vary with time as shown in Figure 2. This boundary condition simulates a time-varying rotation condition provided by a programmable motor. In equation (7), a is the rotation component of the wall velocity, b is the amplitude of oscillations, and ω is the frequency of oscillations.

Based on the oscillation of the wall boundary condition, we can solve for the time-dependent velocity $u_{\theta}(r,t)$ and the shear rate γ within the fluid. The shear rate γ is obtained as

$$\gamma = r \frac{d\left(u_{\theta}/r\right)}{dr} \,. \tag{8}$$

This problem can also be traced to Stokes's second problem in cylindrical coordinates [19]. Here we solve the time-dependent velocity of water numerically using a finite element solver in MATLAB . There are 251 mesh cells uniformly distributed from the center (r=0) to the wall (r=R) and 150,000 time steps. With the flow field known as a function of time, the trajectory of particles within the tank can be determined by also considering their sinking velocity. Here, we assume a constant

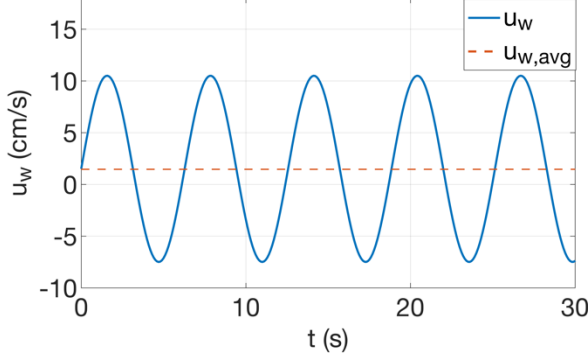


Figure 2. Velocity at the wall in the oscillating roller tank

sinking rate of 5m/day, which is representative of a wide range of particulate matter in the ocean [18]. To calculate stable trajectories, we seed 10,000 particles randomly into the tank and integrate their position through time. The calculation continues until unsteady trajectories are obtained or a simulation time of 15,000 seconds (4.2 hours) is reached. This timeframe was chosen for our simulations since it typically takes 3.5 to 4 hours to complete one experiment of in-lab marine snow preparations [16].

In the turbulent ocean, the shear rate, γ (s⁻¹), is usually calculated based on the energy dissipation rate ε (W kg⁻¹). For turbulent flow, these parameters have the relationship of

$$\gamma = \sqrt{\frac{\varepsilon}{v}}$$
 (9)

For the laminar flow in the roller tank, we can directly calculate the shear rate from the velocity profile according to equation (8). To estimate if the flow within the tank remains laminar, we first define a Reynolds number as

$$Re = \frac{(a+b)R}{v},$$
 (10)

where a+b is the maximum speed at the wall and R is the radius of the roller tank. Determining the critical Reynolds number that causes turbulence is more difficult. High frequencies of oscillation can lead to turbulence in rotating tanks. Borro-Echeverry *et al.* [20] measured the flow field in a cylinder filled with water during an impulsive start condition. Based on their study, a Reynolds number of Re = 6300, defined with the definition in equation (10), is a conservative estimate of when a turbulent flow appears. The impulsive start condition of Borro-Echeverry *et al.* can likely be regarded as a greater disturbance compared with the present oscillating boundary condition. Additional methods to define a critical Reynolds number for this flow are still under consideration.

RESULTS

3.1 Particle Trajectories

Figure 3 shows particle trajectories for different boundary conditions and particle seeding locations. The blue line in the left plots represent the wall of the roller tank, which has a radius of 5 cm. The red point is the initial location of an example particle within the flow as a demonstration. In each case, the tank starts at rest and begins rotating at time t=0. The shaded areas illustrate the stable regions as described in the previous section. A larger stable region is desirable as it will provide more aggregate samples for experimental analysis. The plots on the right are zoomed-in views of the trajectories. Figure 3(a) is the reference trajectory of a randomly-seeded particle inside the standard roller tank design, which rotates with a constant speed. As shown in Figure 3(a), the particle rotates with a near-circular trajectory after an initial transient.

The oscillation frequency used for Figure 3(b), (c) and (d) are 0.02, 0.05 and 1 rad/s, with amplitudes of 0.25, 1 and 9 cm/s, respectively. To verify that the flow remains laminar, only

Reynolds numbers below Re = 6300 are considered as described in Section 2.2. The case shown in Figure 3(b) is an example of an operating condition where the particle failed to reach a stable trajectory, as its starting point was outside of the shaded stable region. In this case, the particle settling velocity is large relative to the rotation speed (Re = 169), which causes it to migrate over

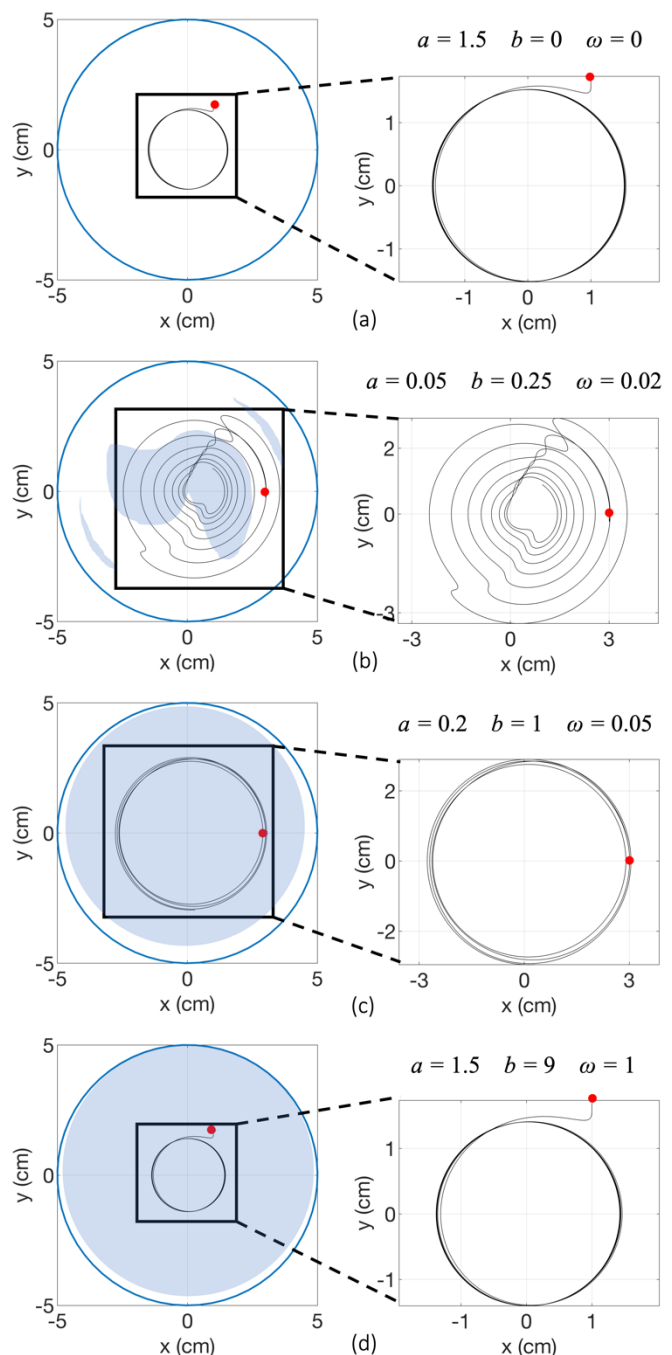


Figure 3. Sample particle trajectories for (a) a constant-rotation-rate roller tank (Re = 843), (b-d) rotating/oscillating roller tanks with Reynolds numbers of Re = 169, 674, and 5898, respectively. The sinking velocity is 5m/d [18], which is a typical value in ocean.

time. In contrast, the trajectories shown in Figure 3(c) and (d) reach a quasi-stable state, where they both achieve a repeatable circular trajectory that does not migrate towards the tank wall. The fractional area of the stable region for the conditions in Figure 3(d) is estimated to be 96.1%, which means 96.1% of particles will not touch the tank wall if the particles are initially uniformly distributed in the roller tank. The stable region for the case in Figure 3(c) is 78.8%, while the stable region shown in Figure 3(b) represents an area of only 35.7% for the time simulated. When the periodic fluid motion is not significantly greater than the sinking velocity of the particles, a greater percentage of the particle trajectories become unstable within the simulation time. The irregular shape of the stable region shown in Figure 3(b) is likely due to the transient nature of the simulation. A longer simulation time leads to smaller stable regions within the tank. It is expected that the stable region for this case will eventually disappear after long periods of time.

The tank wall boundary condition for the results shown in Figure 3(d) are given as

$$u_{\theta}(R,t) = 1.5 + 9 \cdot \sin(t),$$
 (11)

where the maximum velocity on the wall is 10.5cm/s. This boundary condition is also shown in Figure 2. This operating condition is attractive for studying marine aggregates as it exhibits a large stable area and produces relevant shear rates as described in the next section. This operating condition is analyzed further below.

3.2 Velocity profiles and shear rates

In an oscillating system, shear rate varies with velocity profile, which varies with time. Figure 4 displays the tangential velocity profile near the wall in the oscillating roller tank using the boundary condition shown in Figure 2. The velocity magnitude and variation with time decreases rapidly near the center of the roller tank. Most of the variation in velocity is shown to occur in the outer 0.5 cm of the tank.

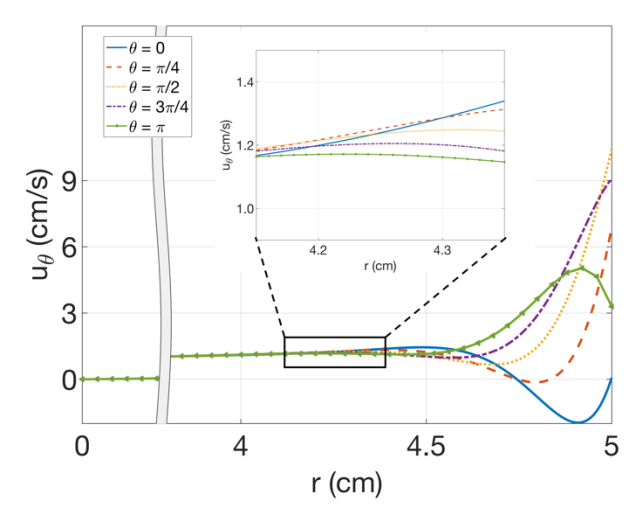


Figure 4. Tangential velocity profiles over time

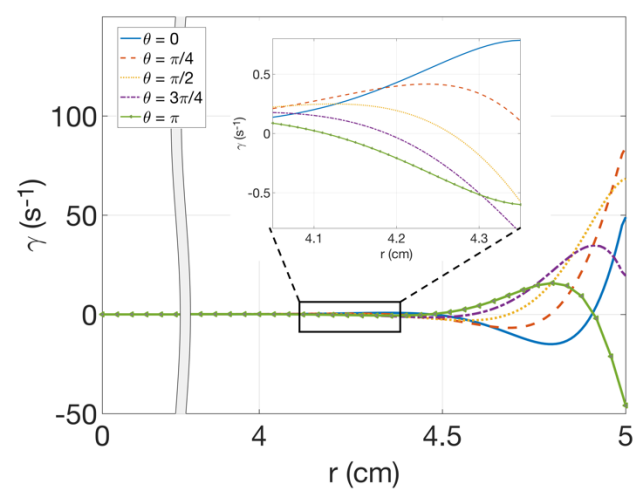


Figure 5. Shear rate profiles over time

Figure 5 displays shear rate calculated from the velocity gradient according to Equation (8). Due to the velocity distributions, the majority of the fluid shear occurs in the outer regions of the cylinder. This means that particles closer to the center of the cylinder will experience less shear, while particles close to the wall will experience higher rates of shear and be more prone to disaggregation.

In the open ocean, the energy dissipation rate (ε) typically varies from 10⁻¹⁰ W kg⁻¹ to 10⁻¹ W kg⁻¹, but can reach 300 s⁻¹ in turbulent surf zones [21]. The operating condition shown in Figure 5 provides shear that is representative of the open ocean and provides a convenient way to expose marine aggregates to a wide range of shear rates. Low values of shear, which occur at radial positions below r = 4.5 cm, are representative of calm areas in the ocean. Higher values of shear, which occur at radial positions above r = 4.5 cm, are representative of shear that particles would experience near the surface in the ocean's mixing layer. Additional operating conditions can easily be created by changing the size of the roller tank diameter or the frequency and amplitude of the boundary oscillations. Further experimental verification is necessary to investigate the limit of the presented boundary conditions and the critical Reynolds number for the transition to turbulence.

Future Work

In order to quantify the breakup strength of an aggregate that disrupts, its exposure to shear needs to be measured. From the numerical calculations presented in this paper, a history of velocity (u_{θ}) and shear rate (γ) is available as a function of radial position (r) in the roller tank and time (t) from the initiation of the tank motion. Optically-clear acrylic roller tanks, combined with a camera measurement system and particle tracking algorithms, will provide time-resolved measurements of the aggregate positions in the tank. This will allow for determination of shear exposure, while also simultaneously capturing the size, shape, and any disruption events that occur. The lack of

measurement probes and pumps within the tank should minimize alterations to the delicate structure of organic marine aggregates (example shown in Figure 6) [22]. This measurement scheme will lead directly to the determination of the aggregate breakup frequency as a function of its size, shape, and shear exposure (*i.e.* defining K in equation (3)). Tracking of breakup mass will also allow for definition of the size-distribution of the disrupted material, or Γ in equation (3). The empirical data of disruption events will be used to inform additional disaggregation models that describe the breakup behavior of organic marine particles for use in the PBE.

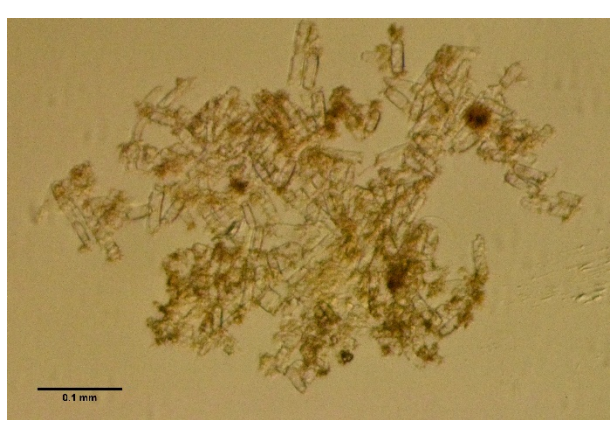


Figure 6. Aggregate of phytoplankton (Odontella Aurita v. Minima, UTEX) cultured in-lab.

CONCLUSIONS

A rotating/oscillating roller tank was analyzed for the study of aggregation and disaggregation of organic marine particles. It was found that stable operating conditions exist at higher Reynolds numbers where the majority of particle aggregates within the flow will not be influenced by the cylindrical tank wall. Operating conditions were identified that provide laminar shear rates that approximate the shear magnitudes expected in the open ocean. Rotating/oscillating roller tanks were found to be a promising experimental method for studying the disaggregation behavior of organic marine aggregates.

ACKNOWLEDGEMENTS

The authors would like to thank Dr. Steven Ackleson of the US Naval Research Lab for technical discussions related to this work.

REFERENCES

- [1] Hsu, J. P., and Glasgow, L. A., 1983, "Floc size reduction in the turbulent environment," Part. Sci. Technol., 1(2), 205-222.
- [2] Smith, S. J., Friedrichs, C. T., 2011, "Size and settling velocities of cohesive flocs and suspended sediment aggregates in a trailing suction hopper dredge plume," Cont. Shelf Res., 31, 50-63.

- [3] Kim, N.-H., 2018, "Particulate fouling and on-line cleaning of ferric oxide particles in internally enhanced tubes, Heat Transf. Eng., 39(1), 40-50.
- [4] Yang, M. Y., Chan, J. G. Y., Chan, H. K., 2014, "Pulmonary drug delivery by powder aerosols," J. Control Release, 193, 228-240.
- [5] Folwer, S. W., and Knauer, G. A., 1986, "Role of large particles in the transport of elements and organic-compounds through the oceanic water column," Prog. Oceanogr., 16(3), 147-194.
- [6] Burd, A. B., and Jackson, G. A., 2009, "Particle aggregation," Ann. Rev. Mar. Sci., 1(1), 65-90.
- [7] Parker D. S., Kaufman, W. J., and Jenkins, D., 1972, "Floc breakup in turbulent flocculation processes," J. Sanit. Eng. Div., 98(1), 79-99.
- [8] Jackson, G. A., 1995, "Comparing observed changes in particle size spectra with those predicted using coagulation theory," Deep Res. Part II, 42(1), 159-184.
- [9] Spicer, P. T., and Pratsinis, S. E., 1996, "Coagulation and fragmentation: Universal steady-state particle-size distribution," AIChE J., 42(6), 1612-1620.
- [10] Saha D., Soos, M., Luthi, B., Holzner, M., Liberzon, A., Babler M. U., and Kinzelbach, W., 2014, "Experimental characterization of breakage rate of colloidal aggregates in axisymmetric extensional flow," Langmuir, 30(48), 14385-14395.
- [11] Kusters, K. A., 1991, "The influence of turbulence on aggregation of small particles in agitated vessels, PhD Thesis, Eindhoven University of Technology.
- [12] Flesch, J. C., Spicer, P. T., and Pratsinis, S. E., 1999, "Laminar and turbulent shear induced flocculation of fractal aggregates," AIChE J., 45(5), 1114-1124.
- [13] Chen W., Fischer, R., and Berg, J., 1990, "Simulation of particle size distribution in an aggregation-breakup process," Chem. Eng. Sci., 45(9), 3003-3006.
- [14] Spicer, P. T., Keller, W., and Pratsinis, S. E., 1996, "The effect of impeller type on floc size and structure during shear-induced flocculation," J. Colloid. Interface. Sci., 184(1), 112-122.
- [15] McCave, I. N., 1984, "Erosion, transport and deposition of fine-grained marine sediments", In: Stow, D. A. V., Piper, D. J. W. (Eds.). Fine-grained sediments: deepwater processes and facies. Blackwell Scientific Publications, Oxford, p. 35-69.
- [16] Shanks, A. L. and Edmondson, E. W., 1989, "Laboratory-made artificial marine snow: a biological model of the real thing", Marine Biology 101, 463-470.
- [17] Jackson, G. A., 1994, "Paricle trajectories in a rotating cylinder: implications for aggregation incubations", Deep-Sea Research 1, Vol. 41, No. 3, pp. 429-437.
- [18] Jackson, G. A., 2015, "Coagulation in a rotating cylinder", Limnology and Oceanography: Methods 13, 2015, 194-201.
- [19] Li, K.W., Marfatia, A. C., 1971, "Stokes Second Problem for the Cylinder", Journal of Basic Engineering, 93(2), 326-328.

- [20] Borrero-Echeverry, D., Schatz M. F. and Tagg R. 2010, "Transient turbulence in Taylor-Couette flow", Physical Review, E81, 025301(R).
- [21] Thorpe S. A., 2015, "The turbulent ocean". Cambridge University Press, p. 25.
- [22] Rau, M. J., Ackleson, S. G., and Smith, G. B., 2018, "Effects of turbulent aggregation on clay floc breakup and implications for the oceanic environment," PLoS ONE, 13(12), e0207809.